A PASSIVELY MODE-LOCKED Cr^{4+}:FORSTERITE LASER WITH ELECTRONICALLY CONTROLLED OUTPUT CHARACTERISTICS FOR NOVEL IMAGING AND MANIPULATION SYSTEMS

Zolotovskaya S. A.[1], Wilcox K. G.[1], Abdolvand A.[1], Livshits D. A.[2], Rafailov E. U.[1]

[1]School of Engineering, Physics and Mathematics, University of Dundee, United Kingdom
[2] Innolume GmbH, Germany

Applicability of electronic control of laser output parameters to bulk solid-state laser sources is demonstrated. A single laser source with variable pulse duration for novel imaging and manipulation systems is presented. Stable passive mode-locking of a Cr^{4+}:forsterite laser using a voltage controlled p-n junction quantum dot saturable absorber was achieved. Output shortening from 17,4 to 6,4 ps near-transform limited pulses was obtained by applying reverse bias.

Introduction

For a number of applications the generation of short pulses is paramount importance. The techniques, commonly used to generate ultrashort optical pulses from tunable solid-state lasers, include active and passive mode-locking. Passive mode-locking of solid-state lasers has made tremendous progress during last decade, following the introduction of three novel techniques: additive-pulse mode-locking [1], Kerr lens [2] and semiconductor saturable absorber (SESAM) [3] mode-locking. Of these, the first two techniques employ quasi-instantaneous third-order optical nonlinearity to create an artificial fast saturable absorber. SESAM mode-locking represents saturable absorbers in the classical sense based on the fast relaxation time of carriers.

The development of SESAMs led to a great improvement in the self-starting, robustness and reliability of ultrashort pulse laser systems. Bandgap engineering has allowed SESAM technology to be applied across a broad spectral range, with many different laser types. Quantum dot-based SESAMs (QD-SESAMs) have been used to assist and sustain passive mode-locking in a variety of solid-state laser systems emitting in the spectral range of 1,0–1,3 μm [4].

Laser sources with controllable output characteristics are of special interest to improve the flexibility of the systems for end users. Electronic control of laser parameters, in particular switching between continuous wave (CW) and pulse-duration-controllable mode-locked operation, is beneficial for novel imaging and manipulation systems [5]. Employment of a single laser source, capable of fast switching between two operational regimes, can also be advantageous for trapping and manipulation of biological objects with subsequent photoporation or dissection [6, 7]. Semiconductor edge emitter laser development has led the way in this, with the laser output controllable by applying a reverse bias to a *p-i-n* saturable absorber section [8, 9]. The concept of a voltage controllable *p-i-n* saturable absorber has also been applied to solid-state lasers, however, with limited success. An electrically-enhanced SESAM-like structure for passive mode-locking of a Ti^{3+}:sapphire laser permitted a degree of control, demonstrating switching between pulses of duration one nanosecond to several hundreds of picoseconds [10]. More recently a QD-based SESAM, with incorporated *p-n* junction, was used to stabilise a passively mode-locked Yb^{3+}:KYW laser under reverse bias voltage conditions [11].

In this paper, a passively mode-locked Cr^{4+}:forsterite laser with electronically controlled pulse duration is demonstrated. A DC voltage controlled *p-n* junction quantum dot semiconductor saturable absorber mirror is presented. Output pulse durations varying from 17,4 to 6,4 ps were obtained by applying a DC voltage between 0 and –4,5 V. No dispersion compensation was used.

Experimental method and sample description

The basic design of a *p-n* junction QD-SESAM structure under investigation is depicted in Figure 1, where the material structure was grown using a conventional solid source MBE technique. The *p-n* junction SESAM structure comprised of, in order, a 300 nm Si-doped GaAs buffer layer deposited on an *n*-type GaAs substrate, an *n*-doped distributed Bragg reflector (DBR) and a 4λ-long GaAs micro-cavity, with a design wavelength of 1260 nm incorporating a *p*-doped GaAs cap layer.

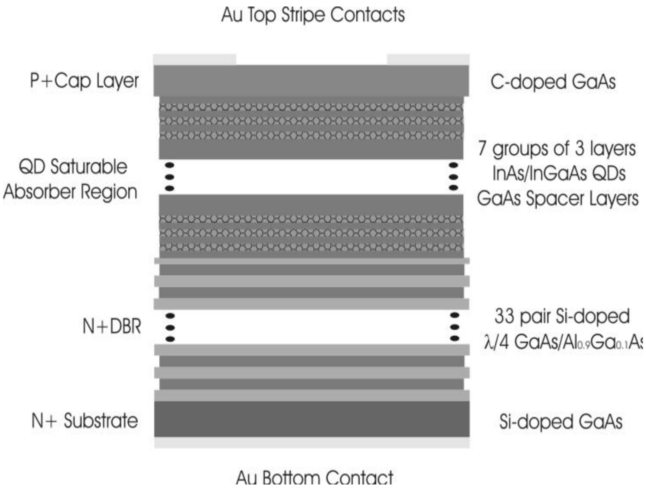

Figure 1 – Structure design of the *p-n* junction QD-SESAM

Metal contacts were deposited on the p- and n-side of the device. The highly reflective DBR consisted of 33 pairs of Si-doped λ/4 $GaAs/Al_{0,9}Ga_{0,1}As$ layers. The QD saturable absorber region was formed in 7 groups consisting of 3 layers of InAs/InGaAs QDs, grown in the Stranski-Krastanow regime, with 32 nm-thick GaAs spacer layers in between. The groups of QDs were positioned at the antinodes of the electric field standing wave using GaAs spacers. The *p*-GaAs cap layer had a doping concentration of approximately NA=2×10^{19} cm^{-3}. Following the growth process, the wafer was thinned to 100 µm and the full area of the *n*-side was metallised with a GeAu/Ni/Au alloy. On the *p*-side, stripe contacts, with a separation distance of ~300 µm were formed with a ZnAu/Au alloy.

The *p-n* junction QD-SESAM was used as a cavity mirror in the laser. The laser output was characterised for applied voltages ranging from 0 to -4,5 V. A schematic of the experimental setup is depicted in Figure 2. An Yb^{3+}:fibre laser (IPG Laser GmbH), producing of up to 10 W of linearly polarised near-diffraction limited light at 1,06 µm, was used as a pump source. A focusing system provided an $1/e^2$ pump spot diameter of ~ 32 µm in the crystal.

The Brewster-cut Cr^{4+}:forsterite crystal had a length of 12 mm and small signal absorption coefficients of 1,11 and 0,007 cm^{-1} at the wavelengths of 1075 and 1250 nm respectively. The crystal was wrapped in indium foil and placed into a copper heat spreader. The crystal boundary temperature of 12 ºC was maintained by thermoelectric cooling. A four-mirror, asymmetric, astigmatically compensated Z-fold cavity design was used which made it possible to maintain an appropriate cavity mode size within the gain crystal and a degree of control over intacavity fluence upon the saturable absorber device.

The two curved folding mirrors (M_2, M_3) had radii of curvature of -75 and -100 mm, for the short and long arms respectively, and were designed for high reflection (HR) in the 1180–1380 nm spectral range. A wedged output coupler (M4) was located at the end of the long arm of the cavity. A flat HR mirror (M_1) or the *p-n* junction QD-SESAM terminated the short arm of the cavity.

Results and discussion

The CW performance of the Cr^{4+}:forsterite laser was characterised with an output coupler transmittance of 1%. A maximum output power of 240 mW was achieved at an incident pump power on the crystal of 6 W. The slope efficiency was calculated to be 10,8 %.

The free-running wavelength of the laser was centered at 1277 nm. Stable mode-locking operation of the Cr^{4+}:forsterite laser with the unbiased *p-n* junction QD-SESAM was obtained with an output coupler transmittance of 1 % when the flat HR end mirror M_1 was replaced with the SESAM device. A pulse sequence corresponding to the laser fundamental repetition rate of 208 MHz, with an average output power of 47 mW, was attained at an incident pump power of 6 W with the unbiased *p-n* junction QD-SESAM.

Figure 3 (a) represents a typical autocorrelation trace acquired from the passively mode-locked Cr^{4+}:forsterite laser in this regime, measured with a free-space autocorrelator (FR-103XL, Femtochrome Research Inc.) utilizing background free (non-collinear) second harmonic generation.

The output pulse duration was deduced to be 17,4 ps at full-width half-maximum (FWHM), assuming a Gaussian intensity profile.

An optical spectrum of the mode-locked Cr^{4+}:forsterite laser, depicted in Figure 3 (b), had a slightly asymmetrical shape for the long-wavelength wing and was centred at a wavelength of 1280 nm, with a spectral width of 0,3 nm at FWHM.

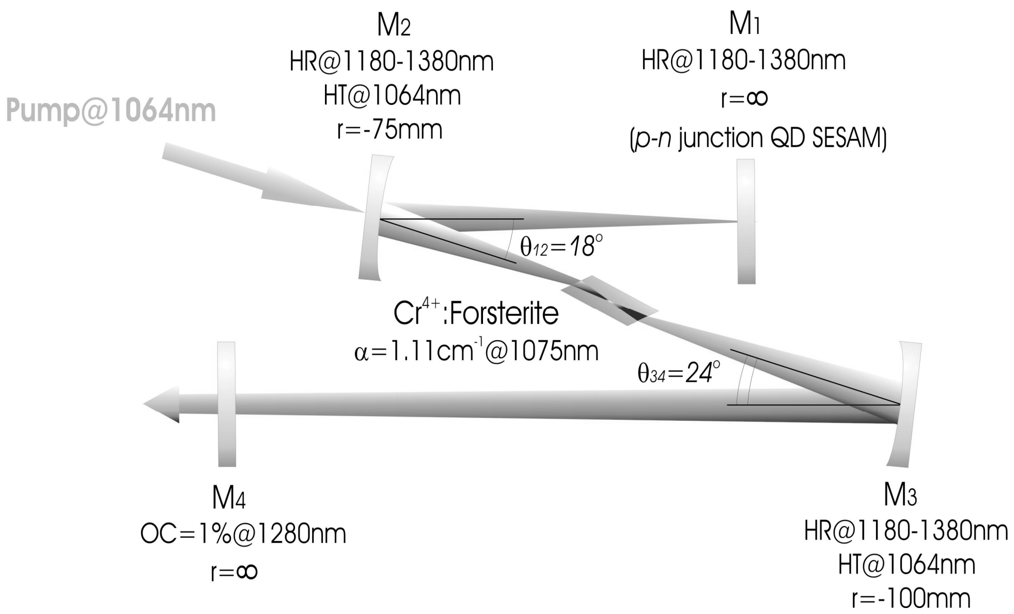

Figure 2 – Schematic of the Cr^{4+}:forsterite laser cavity

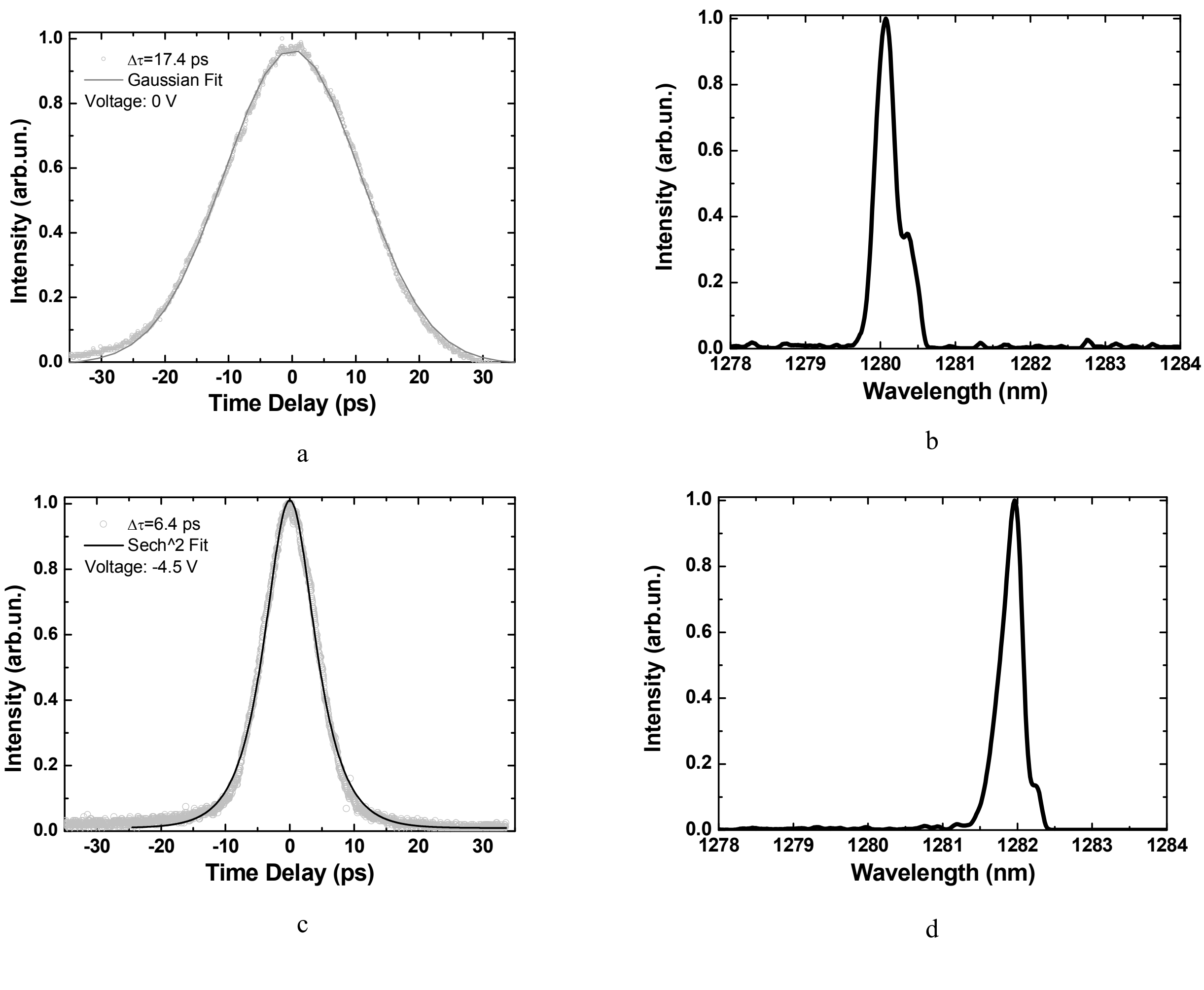

Figure 3 – Intensity autocorrelation trace of the pulses and optical spectra obtained from the Cr^{4+}:forsterite laser with voltage 0 V (a, b) and -4.5 V (c, d) applied on the *p-n* junction QD-SESAM

A DC reverse bias on the *p-n* junction QD-SESAM was applied for voltages from zero to –4,5 V in the same experimental setup and for the same pumping conditions. The effect this reverse bias had on the mode-locked behaviour of the laser was investigated. Stable mode-locked operation of the Cr^{4+}:forsterite laser was attained across the whole bias range with pronounced pulse shortening observed with increasing applied reverse voltage. The shortest pulses achieved had duration of 6,4 ps FWHM, with a $sech^2$ intensity profile, when the *p-n* QD-SESAM was under a bias voltage of -4,5 V, as represented in Figure 3 (a). The average output power from the mode-locked laser, under the -4.5 V bias conditions, was measured to be 29 mW. The calculated pulse fluence upon the QD device was ~400 μJ/cm^2. The observed spectral width of 0,32 nm, at a centre wavelength of 1282 nm, as shown in Figure 3 (b), yielded a close to Fourier-limited time-bandwidth product of 0,37. The decrease in average output power from 47 mW, attained with unbiased QD-SESAM mode-locking, to 29 mW, obtained from the Cr^{4+}:forsterite laser with voltage -4,5 V applied on the *p-n* junction QD-SESAM, was attributed to DC electro-absorption [12, 13], contributing as additional nonsaturable loss introduced in the SESAM structure at higher bias. A red-shift of mode-locked Cr^{4+}:forsterite laser central operating wavelength observed with an increase in applied reverse bias on the p-n junction QD-SESAM. A 2 nm detuning, associated with changes in the SESAM operating conditions under reverse bias, results from interplay between changes in the refractive index, due to changes in carrier density, and heating of the saturable absorber structure. Previously reported field dependent refractive index change for a broadband transmission measurements in the 1,3 μm region in a *p-i-n* InAs dot-in-a-well waveguide modulator, for a range of reverse bias (0–10 V), revealed the refractive index change of 0,001 [14]. A different pulse intensity profile, i.e. Gaussian for 0 V reverse bias on the SESAM structure and $sech^2$ for an applied bias of –4,5 V, indicates the presence of high-order dispersion in the laser cavity for the unbiased SESAM configuration.

The pulse width shortening of the passively mode-locked Cr^{4+}:forsterite laser obtained with an increase in applied reverse bias on the *p-n* junction QD SESAM is shown in figure 4. It should be noted that no reduction in the pulse duration was observed at low reverse bias. The absence of the experimental data in the bias range from –0,5 to –2,5 V was associated with non-uniform injected carrier distribution in the lateral direction in the *p*-doped cap layer of the *p-n* junction SESAM device. It is thought to be due to the lower mobility of holes than electrons and significant distance between the top contacts.

A clear exponential decrease in the slow component of the characteristic recovery time of semiconductor saturable absorbers has been observed in a number of material structures with increasing reverse bias. Recovery time shorting to 700 fs has been measured in a *p-i-n* InAs dot-in-a-well waveguide structure at 1,28 μm with an applied reverse bias of 300 kV/cm at room temperature [13]. An exponential-like decrease of the mode-locked pulse width with increasing reverse bias on the absorber section in a two-section InGaAs QD laser diode was demonstrated and attributed to the exponential dependence of the absorber recovery time on applied reverse bias [15]. A reduction in the simulated pulse duration from 8 to 3 ps, corresponding to about 2,7 times mode-locked pulse duration shortening, was observed for absorber lifetime reduction from 40 to 20 ps for multi-section laser diode implementations [16]. These may suggest that the experimentally observed 2,7 times reduction in the mode-locked pulse duration is dominated by a decrease in the saturable absorber recovery time under reverse biasing which should lead to a voltage-dependent pulse shortening with a characteristic exponential decay. The exponential fit to the experimental data obtained, presented as solid curve in Figure 4, appears to confirm the proposed pulse shortening mechanism.

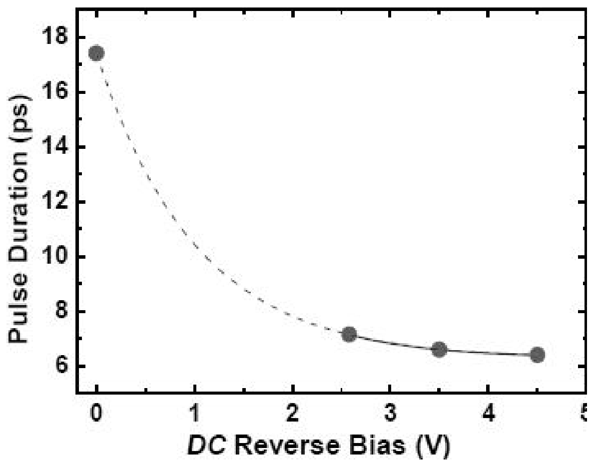

Figure 4 – Mode-locked pulse width shortening (dots) obtained with an increase in applied reverse bias on the *p-n* junction QD-SESAM. The line is a proposed exponential fit

It is anticipated that a reduction in mode-locked pulse duration can in principle lead to an exponential decrease of the pulse width in the low reverse bias range, depicted as a dashed curve in Figure 4. However further investigation of the pulse shortening at low bias voltages and studies of field-enhanced nonlinear optical properties of the SESAM device are required in order to define the dominant pulse shortening mechanism.

It should be mentioned that the minimum pulse duration of 6,4 ps was acquired from the mode-locked Cr^{4+}:forsterite laser with no intracavity dispersion compensation. Figure 5 shows the calculated DBR reflectivity spectrum, group delay dispersion (GDD) and longitudinal confinement spectrum at the SESAM design wavelength of 1260 nm for the spectral range of 1180–1350 nm.

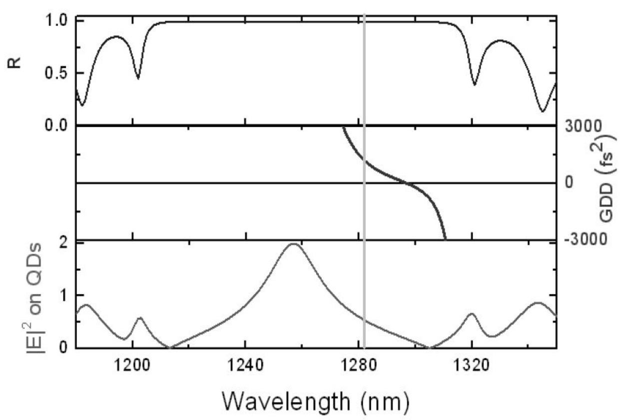

Figure 5 – Calculated DBR reflectivity (R), group delay dispersion (GGD) and longitudinal confinement factor spectrum ($|E|^2$) of the *p-n* junction QD-SESAM used. The vertical line indicates the Cr^{4+}:forsterite central operating wavelength

The DBR reflectivity spectrum shows the flat-topped stop-band of about 100 nm wide typical for the $GaAs/Al_{0,9}Ga_{0,1}As$ DBR, with index contrast of about 0,5. The longitudinal confinement factor exhibits a sharp resonance peak, determined by the thickness of the structure and the reflectivity of the boundary surfaces. The presence of strong GDD, caused by the SESAM micro-cavity being close to resonance, can also be seen. The Cr^{4+}:forsterite lasing wavelength lies at a long wavelength wing of the SESAM resonance with a SESAM induced GDD of approximately +2000 fs^2 per pass. Although introduction of adequate intracavity dispersion compensation would lead to further reduction of the pulse duration, it was not feasible to achieve the necessary level of negative GDD to balance positive dispersion introduced by the SESAM in the present cavity configuration. Moreover the optical bandwidth of the resonant SESAM structure, available for mode-locking, appears to be limited and would also contribute as a spectral filtering element, determining the minimum achievable pulse duration from the passively mode-locked laser system.

Conclusions

In conclusion, the operation of a *p-n* junction QD-SESAM, and its effects on the mode-locked pulse duration of the Cr^{4+}:forsterite laser was investigated in the 1,3 μm spectral range. Stable mode-locking was achieved when the *p-n* junction QD-SESAM was both unbiased and biased. A 2,7 times reduction in pulse duration, producing near-transform limited pulses of duration 6,4 ps for applied reverse bias of 4,5 V, was demonstrated for the first time in a solid-state bulk laser system. The proposed electronic control of solid-state laser characteristics could be beneficial for novel imaging and manipulation systems. The results also suggest that the fast switching, limited by the carrier mobility and carrier recombination time, can be obtained.

References

1. *Ouellette, M. P.* Pulse shaping and passive mode-locking with a nonlinear Michelson interferometer / M. P. Ouellette // Opt. Commun. – 1986. – № 60, – P. 99–103.
2. *Spence, D.E.* 60-fsec pulse generation from a self-mode-locked Ti:sapphire laser / D.E. Spence, P. N. Kean, W. Sibbett // Opt. Lett. – 1991. – № 16, – P. 42–44.
3. *Keller, U.* Broadband fast semiconductor saturable absorber / Keller U. [et al.] // Opt. Lett. – 1992. – Vol. 17.– P. 505–507.
4. *Lagatsky, A. A.* Ultrashort-pulse lasers passively mode locked by quantum-dot-based saturable absorbers / Lagatsky A. A. [et al.] // J. Progress in Quantum Electronics. – 2010. – № 34, – P. 1–45.
5. Agate, B. Femtosecond optical tweezers for in-situ control of two-photon fluorescence / Agate B. [et al.] // Opt. Exp. – 2004. – № 12, – P. 3011–3017.
6. *Stevenson, D.* Femtosecond optical transfection of cells: viability and efficiency / Stevenson D. [et al.] // Opt. Exp. – 2006. – № 14, – P. 7125–7133.

7. *Ando, J.* Optical trapping and surgery of living yeast cells using a single laser / Ando J. [et al.] // Rev. Sci. Instrum. – 2008. – № 79, – P. 103705.
8. *Thompson, M. G.* Regimes of mode-locking in tapered quantum dot laser diodes / M. G. Thompson, R. V. Penty, I. H. White // Proc. IEEE 21st Int. Semiconductor Laser Conf. 2008, Sorrento, Italy, – P. 27–28.
9. *Rafailov, E. U.* High-power picosecond and femtosecond pulse generation from a two-section mode-locked quantum-dot laser / Rafailov E. U. [et al.] // Appl. Phys. Lett. – 2005. – № 87, – P. 081107-1.
10. *Stormont, B.* Extended-cavity surface-emitting diode laser as active mirror controlling modelocked Ti:sapphire laser / B. Stormont [et al.] // – Electron. Lett. – 2004. – № 40, – P. 732–734.
11. *Lagatsky, A. A.* Quantum-dot-based saturable absorber with p-n junction for mode-locking of solid-state lasers / A. A. Lagatsky [et al.] – IEEE Photon. Technol. Lett. – 2005. – № 17, – P. 294–296.
12. *Malins., D. B.* Ultrafast electroabsorption dynamics in an InAs quantum dot saturable absorber at 1.3μm / D. B. Malins. [et al.] // Appl. Phys. Lett. – 2006. – № 89, – P. 171111-1.
13. *Karin, J. R.* Ultrafast dynamics in field-enhanced saturable absorbers / J. R. Karin [et al.] // Appl. Phys. Lett. – 1994. – № 64, – P. 676–678.
14. *Malins, D. B.* Electro-absorption and electro-refraction in an InAs quantum dot waveguide modulator / Malins D. B. [et al.] // IEEE Photon. Technol. Lett. – 2007. – № 19, – P. 1118–1120.
15. *Thompson, M. G.* Subpicosecond high-power mode locking using flared waveguide monolithic quantum-dot lasers / M. G. Thompson [et al.] // Appl. Phys. Lett. – 2006. – № 88, – P. 133119.
16. *Yang, W.* Study of passive mode locking of semiconductor lasers using time-domain modeling / W. Yang, A. Gopinath // Appl. Phys. Lett. – 1993 – № 63. – P. 2717.

Золотовская С. А., Вилкокс К. Г., Абдольванд А., Лившиц Д. А., Рафаилов Э.У.

Электронный контроль выходных параметров лазера на основе кристалла Cr^{4+}:форстерит с пассивной синхронизацией мод для новых систем формирования изображения и манипуляции

Показана возможность применения электронного контроля выходных параметров твердотельных лазерных источников излучения. Демонстрируется одиночный лазерный источник с варьируемой длительностью импульса для новых систем формирования изображения и оптической манипуляции. Стабильная пассивная синхронизация мод лазера на основе Cr^{4+}:форстерит была достигнута с применением квантово-точечного насыщающегося поглотителя с *p-n* переходом, контролируемым посредством приложения напряжения. Сокращение выходных импульсов от 17,4 до 6,4 пс было достигнуто за счет приложения обратного смещения к *p-n* переходу.

Поступила в редакцию 23.02.2011.